ELSEVIER

Journal of Molecular Catalysis B: Enzymatic 1 (1996) 191–199

JOURNAL OF MOLECULAR CATALYSIS B: ENZYMATIC

Effect of a charged residue at the 213th site of thermolysin on the enzymatic activity

Yoichiro Miki [a,1], Shun-ichi Kidokoro [a,*], Kimiko Endo [a], Akiyoshi Wada [a], Takashi Yoneya [b], Atsuo Aoyama [b], Kenichi Kai [b], Toshio Miyake [b], Hiromasa Nagao [b]

[a] *Sagami Chemical Research Center, Nishiohnuma 4–4–1, Sagamihara, Kanagawa 229, Japan*
[b] *Biotechnology Research Laboratory, TOSOH Corp., Hayakawa 2743-1, Ayase, Kanagawa 252, Japan*

Received 27 October 1995; revised 31 January 1996; accepted 7 February 1996

Abstract

Considering the electrostatic potential of active site, four mutants of thermolysin (EC 3.4.24.4) are designed in an attempt to change the optimum pH of the hydrolytic activity toward acidic regions. On the basis of the numerical calculation of the electrostatic potential in the thermolysin molecule, Asp213 is targeted to be replaced by a basic residue, His, Lys, Arg or a neutral one, Asn. The mutant enzymes are produced in *Bacillus subtilis* as a host using the method of site-directed mutagenesis and their optimum pH values for hydrolyzing a synthetic substrate furylacryloyl–Gly-L-Leu–NH_2 are found to be lowered by 0.2–0.4 pH units with reference to the wild type enzyme. The pI shifts of the mutants are evaluated. Neither optimum pH nor pI shift can be explained by the contribution of the pK change only at the mutation site. We find a clear negative correlation between the activities at pH 7.0 and the pI values among the four mutants and wild-type enzyme. It suggests that the contribution of pK shift of other residues must be taken into account in order to explain the activity change. Little change of thermal stability is observed among the mutants and wild type enzymes.

Keywords: Thermolysin; Activity; Electrostatic potential; Optimum pH; pI

1. Introduction

Thermolysin (EC 3.4.24.4) is one of the most interesting enzymes both in scientific and practical fields, because of its extremely high thermal stability and relatively narrow specificity [1,2]. Its amino acid sequence [3,4] and three-dimensional structure to 1.6 angstrom resolution [5] has been solved. The thermal stability has been explained in terms of its structure [5], while four calcium ions have also been revealed to be essential for the structural stability [6]. The mechanism of catalysis was proposed through the crystallographic studies of substrate–thermolysin complexes [7–11].

A number of neutral proteases which are homologous to thermolysin are known. Some of their genes have been cloned [12–16] and several studies on the structure–function and structure–stability relationships have been done by means of site directed mutagenesis [17–22]. The

* Corresponding author.
[1] Present address: Nagaoka University of Technology, Department of BioEngineering, Nagaoka, Niigata 940-21, Japan.

PII S1381-1177(96)00006-9

structural gene of thermolysin has been cloned from two closely related microorganisms: *Bacillus stearothermophilus* [13] and *B. thermoproteolyticus rokko* [23,24]. In fact, it was shown that the two genes are identical both in the nucleotide sequence and in the amino acid sequence of the product protein [25].

There are several possible approaches to clarify the structure–function relationship lying in protein molecules by protein engineering. We aimed to control the pH-dependence of the activity of thermolysin, because this has practical as well as scientific meanings: it is useful if the optimum pH can be shifted toward the acidic region so that the enzymatic reaction can be achieved in an industrial process. One of the most important industrial applications of thermolysin is its use in the enzymatic synthesis of aspartame, such as, for instance, being practiced at Holland Sweetener Company (a joint venture company of TOSOH and DSM). The methyl esters of the materials are more stable in weakly acidic pH than at the optimum pH of thermolysin.

In order to change the optimum pH, we must select the target residues to be mutated, which are expected to affect the electrostatic environment of the active site. We do not change the residue(s) of the active site directly, as their replacement would have a fatal effect on the activity.

The protonation–deprotonation equilibrium of an ionizable residue depends on the electrostatic potential at the residue itself. The midpoint of protonation–deprotonation state, i.e. pK, is shifted toward lower pH if the electrostatic potential is raised, and vice versa [26–28]. Thermolysin shows the highest activity at the neutral pH, which is presumably determined by the protonation states of the two residues at the active site, Glu143 and His231: the condition where thermolysin is active is that Glu143 is deprotonated to have a negative charge and His231 is protonated to have a positive charge. Both the deprotonated form of Glu143 and the protonated form of His231 are expected to provide the transition-state stabilization for the enzymatic reaction.

In previous papers [29,30], we have reported the highly activated mutants on the mutation site where the amino acid replacement is expected to affect the electrostatic environment at Glu143. Negative correlation between the activity and the thermal stability was observed. In this paper, we focused on the mutation site which is expected to affect the electrostatic potential around His 231. It was found that the present mutants show an interesting correlation between their physical property and activity while the mutants may not be useful for the direct industrial application.

Our strategy is: (1) to find the most influential residues on His231, based upon the numerical calculation of the electrostatic potential in thermolysin; (2) to introduce a positive charge at one of these residues by site-directed mutagenesis to raise the electrostatic potential at His231, and (3) to evaluate the structure–function relationship precisely [30].

2. Materials and methods

2.1. Protein engineering of thermolysin

The mutagenesis of Asp213 of thermolysin was performed by using the M13 phage mutagenesis method [31]. The plasmid pUCTZ55 was prepared from the plasmid pMK1 [32], which was the expression plasmid of *npr*M in *B. subtilis*, by digesting with *Pst*I and *Bam*HI and by cloning the 3.5 kb fragment into the plasmid pUC9.

The single-stranded template DNA was prepared by cloning the 550 bp fragment obtained by digestion of pUCTZ55 with *Sph*I and *Bcl*I, into phage M13mp18. The mutagenic oligonucleotides used for the replacement of the 213th residue are shown in Table 1. The mutagenesis reaction was performed by using the T7-GEN in vitro mutagenesis kit (United States Biochemicals). The mutations were confirmed by se-

Table 1
Sequences of the mutagenic oligonucleotides [a]

D213N	5′AAGTATGGT*AATC*CAGATCAC3′
D213H	5′AAGTATGGT*CATC*CAGATCAC3′
D213K	5′AAGTATGGT*AAAC*CAGATCAC3′
D213R	5′AAGTATGGT*CGTC*CAGATCAC3′

[a] The triplets for the 213th residues are in italics.

quencing each of the phage DNAs prepared from a number of mutant plaques.

The double-stranded DNA of the mutated M13 phage was excised with *Sph*I and *Aat*I and used to replace the corresponding region of the plasmid pUCTZ55.

A large fragment of pMK1 digested with *Bam*HI and the plasmid pUCTZ55(mutant) digested with *Bam*HI were ligated and directly used to transform the *B. subtilis* MT-2 strain. Kanamycin resistant colonies were selected on LC agar plate (10 g/l Bactotryptone, 5 g/l yeast extract, 5 g/l NaCl, 10 g/l casein and 7 g/l agar). Secretion of mutant thermolysins was detected by halos around colonies.

The recombinant *B. subtilis* (mutant) was stored at −80°C with 20% of glycerol. For getting mutant thermolysin, the recombinant *B. subtilis* was inoculated into 2 × L medium (20 g/l of Bactotryptone, 10 g/l of Yeast extract and 5 g/l of NaCl, pH 7.0) in several culture flasks. During 20 h cultivation at 37°C and 200 rpm, the mutant thermolysin was secreted into the culture medium.

The culture broth was centrifuged at 8000 rpm for 30 min to remove bacteria, and ammonium sulfate was added to the supernatant to attain 60% saturation. The precipitate was recovered by centrifugation to give crude enzyme.

2.2. Purification of mutant enzymes

Each crude sample was purified on an open column (7 mm ID × 12 cm) packed with a hydrophobic interaction chromatography support Butyl–Toyopearl–650S (TOSOH). The column was eluted with 20 mM Tris/HCl buffer (pH 9.0) containing 10 mM $CaCl_2$ at the flow rate of about 2 ml/min. The fractions with the hydrolytic activity against casein were combined, and the protein was precipitated with 60% saturation of ammonium sulfate. The sample was further purified with a gel filtration column G2000SW (21.5 mm ID × 30 cm, Tosoh) eluted with 20 mM Tris/HCl buffer (pH 7.5) containing 10 mM $CaCl_2$ at the flow rate of 2 ml/min. In order to prevent the autolysis, zinc-chelating reagent *o*-phenanthroline (Aldrich) was added immediately to the fractions and the sample solution was stored at 4°C. The solution condition was changed with an ultrafiltration device Centriprep-10 (Amicon) immediately before use. The purity of the sample was checked to be a single band with the isoelectric focusing gel IEF4-6.5 on the PhastSystem (Pharmacia LKB). The concentration of mutants was determined optically assuming that the molar extinction coefficient at 280 nm is 6.63×10^7 cm^2 mol^{-1} that was obtained for the wild type [33].

2.3. Measurement of the hydrolytic activity against FAGLA

We have developed an automated enzyme assay system which comprises an ultraviolet spectrophotometer UB35 (JASCO) and a personal computer PC-9801 (NEC) to store the data. For the measurement of the hydrolytic activity of thermolysin and its mutants, a chromogenic synthetic substrate, furylacryloylglycyl-L-leucine amide (FAGLA) (Bachem) was used in the present study. FAGLA was dissolved in 0.2 M Tris/maleate buffer containing 10 mM $CaCl_2$ at various pH. 2 ml of the FAGLA solution was pre-incubated in a cuvette at 37°C for 5 min. The stock enzyme solution was 20 mM Tris/HCl buffer, pH 7.5, containing 10 mM $CaCl_2$ and 0.2 mM *o*-phenanthroline. The 20 μl zinc solution (5 mM $ZnSO_4$) was added to the 200 μl of the enzyme solution and pre-incubated for 5 min. The solution was added to the FAGLA solution in the cuvette

under stirring to start the enzyme reaction. The final concentration of FAGLA was 1.8 mM and that of the enzyme was varied from 0.05 μM to 0.2 μM for the efficiency of the analysis. The time evolution of decomposition of FAGLA was monitored at 345 nm, where the molar extinction coefficient difference is -3.17×10^5 cm^2 mol^{-1} [34]. The data were analyzed systematically to give the kinetic parameter k_{cat}/K_m [29]. No dependence of enzyme concentration was observed for determining the enzymatic parameter under the present condition.

2.4. Determination of the isoelectric point

The isoelectric point, pI, of the enzymes was determined using an automated gel electrophoresis system, PhastSystem (Pharmacia LKB), with the isoelectric focusing gel plate IEF4-6.5. The sample buffer condition was the same as used for the measurement of the hydrolytic activity. 1 μl each of the samples was loaded on the gel plate with 8-well applicator. After the electrophoresis, proteins were fixed with 20% (w/v) trichloroacetic acid and stained with 0.02% Coomassie Brilliant Blue R250 (Sigma) containing 0.01% $CuSO_4$. The pI value of each sample was determined by interpolation with reference to the pI standard proteins (Pharmacia LKB): glucose oxidase (4.15), soybean trypsin inhibitor (4.55), β-lactoglobulin A (5.20), bovine carbonic anhydrase B (5.85) and human carbonic anhydrase B (6.55), pI values being indicated in the parentheses.

2.5. Measurement of the thermal stability

The thermal denaturation of the enzymes was measured on the differential scanning calorimetry device, MCS (MicroCal). Because the denaturation of thermolysin follows an irreversible process and the thermal transition depends on the heating rate, we define the index of the thermal stability with the peak temperature of the transition curve, Tp, obtained by raising the sample temperature from 10°C to 105°C at the rate of 1 K/min [29]. The sample buffer used was 50 mM HEPES (pH 8.28) containing 10 mM $CaCl_2$ and 0.1 μM $ZnSO_4$. The concentration of the sample was typically about 0.5 mg/ml.

3. Results and discussion

3.1. Calculation of electrostatic potential in the thermolysin molecule

The electrostatic potential in the thermolysin molecule was calculated numerically [35,36] using its atomic coordinates which are available from the Brookhaven Protein Data Bank with the entry code 3TLN [5]. The FORTRAN program that was kindly given by Dr. Haruki Nakamura [35] was transferred to and executed on the workstation Titan 750 (Kubota Computer).

We have used an efficient technique by which the CPU time is drastically reduced. If we check how large each of the residues affects the electrostatic potential around the active site, 315 sets of calculations should naively be performed (there are 316 residues in thermolysin), which requires far too much CPU time. This can be drastically reduced by using the Green's reciprocity theorem [36]. According to it, the following relationship holds between charges i and j:

$$\varphi_i(r_j) = \frac{q_i}{q_j}\varphi_j(r_i)$$

where $\varphi_i(r_j)$ is the potential at the position of charge j produced by the charge i, and q_i is the quantity of the charge i, etc. This relationship implies that the contribution of one charge to the electrostatic potential at the other one can be obtained by calculating inversely the electrostatic potential produced by the latter at the former's position. Therefore, only a single set of calculation is needed, where charges are put on the atoms of His231 alone and all the other charges are set to zero.

The most effective charge that maximizes $\varphi_i(r_j)$ should maximize the product, $q_i\varphi_j(r_i)$, because q_j is the common value. We calculate each product for 315 residues. Using the results of calculation, we made a list of electrostatic contribution of each of the 315 residues to His231.

One large negative contribution by Asp213 is recognized in the procedure mentioned above. This position is completely exposed to the solvent, so it would seem easy to change any large amino acid such as Arg. We thought it of interest to replace this site with a positive or a neutral amino acid, His, Lys, Arg and Asn to change the electrostatic potential on this active site.

3.2. Electrostatic effect of replacement of Asp213 (calculation)

To study the electrostatic influence of the replacement of Asp213 to His, Lys, Arg or Asn, we estimated the pK shifts of all the other ionizable residues, which should be caused by the change of electrostatic potential around them. The coordinates of the mutated residues were estimated using energy minimization with a program QUANTA/CHARMm (Molecular Simulation) on IRIS 4D/80GT (Silicon Graphics) fixing the coordinates of all the other residues.

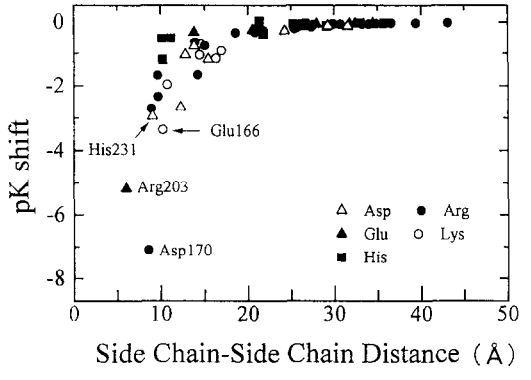

Fig. 1. pK shift vs. distance. For all the ionizable residues, except Lys213 itself, in the mutant D213K, the calculated pK-shifts are plotted against the distances from Lys213. The types of the amino acids are indicated with symbols: Asp (△), Arg (·), Glu (▲), Lys (○) and His (■). The points for Glu166, Asp170, Arg203 and His231 are labeled in the figure.

For all these mutant and wild-type molecules and for all the ionizable residues, protonation energy $E^m(i)$ were calculated, where i and m denote an ionizable residue and the mutant species, respectively: for example, i represents His 231 and m represents the mutant D213H The protonation energy is estimated as the product of obtained electrostatic potential at the ionizable residue and its charge difference between ionized and not-ionized states. Difference of the protonation energy of residue i between wild-type and a mutant m, $E^m(i) - E^{wt}(i) = \Delta E^m(i)$, directly relates to the pK shift, ΔpK, of residue i caused by the mutation of residue m [37] as:

$$\Delta pK^m(i) = -\frac{1}{\ln 10}\frac{\Delta E^m(i)}{RT}$$

Fig. 1 shows ΔpK vs. the distance d between Lys213 and the specified residue for the D213K mutant. The distance is calculated using the center of mass of each side chain. Since +2 charge is introduced at the 213th site, pK shifts are negative for almost all residues. It should be noted that the replacement of Asp213 to Lys largely affects some ionizable residues as well as His231. As all these residues are located within a short range from Lys213, this relationship between d and ΔpK is reasonable, since ΔE is approximately proportional to $1/d$ for those residues which are very close to the 213th residue. Among these residues the largest effects are exerted on Asp170, Arg203 and Glu166. It is known that Glu166 and Asp170 interact indirectly with active site: Glu166 coordinates to the zinc ion which is essential for the activity and Asp170 makes a hydrogen bond with His142 which coordinates to the zinc ion [5,38].

We found that the tendencies mentioned above are almost the same for the other mutants (data not shown) and that there are quantitatively some differences between them. As shown

Table 2
pK-shifts of Asp170 (calculation)

Mutant	ΔpK [a]	d [b]
D213N	2.4	9.6
D213H	4.6	9.5
D213R	6.0	8.8
D213K	7.1	8.6

[a] pK-shift of Asp170 caused by the substitution of Asp213.
[b] Side-chain–side-chain distance between the 213th residue and Asp170 (Å).

in Table 2, the order of ΔpK(Asp170) for them is:

D213N < D213H < D213R < D213K

It is intuitively clear that ΔpK(Asp170) for the three basic-amino-acid mutants are larger than that for D213N because the former are added two units of charge at the mutation site while the latter has only one additive positive charge. The order among the basic-amino-acid mutants is also consistently explainable by considering the distance d (Table 2, column 3): as the side chain of the 213th residue protrudes into the proximity of Asp170 and the charge is located at the end of the chain, the residue with a longer side chain has a larger effect on Asp170. The same discussion is relevant to the relationship between d and pK shift for Arg203, Glu166 and His231 and the order of the estimated electrostatic effect is the same around these four sites (data not shown). These sites are displayed with the mutated residue in Fig. 2.

3.3. pH dependence of hydrolytic activity

For all the mutants and wild-type enzyme, we measured the activity to hydrolyze FAGLA at various pH. Fig. 3 compares the pH-dependence of the activity which is represented by the kinetic parameter k_{cat}/K_m. Statistical error in the parameter obtained is within 1% or less [29]. The pH-profiles of the activity are similar in shape with reduced amplitude for these mutant enzymes. It should be noticed that the optimum pH is successfully lowered in all these mutants: the shifts are 0.4 pH-units for D213H and 0.2 units for the others, D213N, D213K and D213R. The order of the optimum pH shift, however, does not correlate to the estimated electrostatic effect discussed above.

Another characteristic noticeable in Fig. 3 is the degree of reduction of activity. The order of the activity at the neutral or higher pH region is D213H < D213R < D213K < D213N < wild-

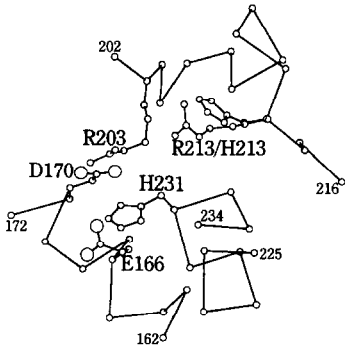

Fig. 2. Three-dimensional structure around the 213th site. The 213th His (H213) of D213H mutant and the 213th Arg (R213) of D213R mutant are illustrated with some other residues which appear in the text: the 166th Glu (E166), the 170th Asp (D170), the 203rd Arg (R203) and the 231st His (H231). Three backbone fragments that contain these residues are also plotted. Only α-carbons are shown for the backbone chains. The structure was estimated from the wild type structure using energy minimization (see text for details).

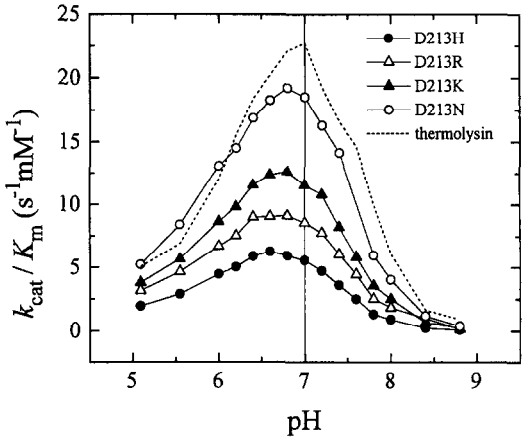

Fig. 3. pH-dependence of activity. Kinetic parameters, k_{cat}/K_m, in hydrolyzing the synthetic substrate furylacryloyl-glycyl-L-leucine amide (FAGLA) at various pH are plotted. The reaction condition is: 1.8 mM FAGLA in 0.2 M Tris/maleate buffer at various pH, containing 10 mM $CaCl_2$; concentration of protease ranges from 0.05 μM to 0.2 μM; temperature is 37°C.

type. The reduction of activity is related to the shift of the optimum pH: those mutant enzymes with the lower optimum pH have the lower activity. In addition, it is noticeable that the activity of D213H is enhanced in the lower pH region in comparison to the wild-type enzyme.

3.4. Comparison of the pI shifts

Table 3 lists the experimental values of pI of the mutants, which were determined by interpolation with reference to the pI markers. We have found that the pIs of all the mutants are shifted toward higher pH. The order of the pI shifts relative to the wild type is D213N < D213K < D213R < D213H. It is reasonable that the pI shift of D213N is the smallest, because the charge difference is smallest in D213N. The order of the pI shifts among the three mutants, D213K, D213R, D213H, however, can not be explained by the simple model assuming that all the pK values of the ionizable residues are not changed by the mutation.

This difference between the observation and the calculation suggests that pK_s of some residues are affected by the mutation at the 213th site. One of the residues whose pK_s are expected to be affected is Asp170. Since the influence of the mutation from D213 to Lys is estimated to be the largest among the mutants (Table 2), the pK of Asp170 of D213K may be the smallest. Among the three basic-amino-acid mutants (D213H, D213R, D213K), the smallest pK may indicate the smallest pI. It suggests that the order of the pIs of these mutants is D213K < D213R < D213H: the order is the same as the experimentally observed among these mutants (Table 3).

Table 3
Calculated and observed values of pI

	pI_{obs}	pI_{calc}
wild type	4.97	5.03
D213N	5.04	5.17
D213K	5.23	5.33
D213R	5.27	5.33
D213H	5.31	5.30

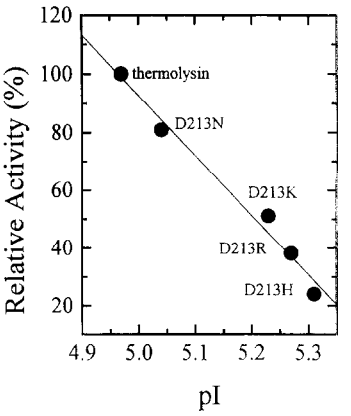

Fig. 4. Correlation between pI and activity. The measured pI values are plotted against the relative hydrolytic activity against FAGLA at pH 7.0 for each enzyme. The activities are indicated in percentage with reference to that of wild-type thermolysin. The linear fitting revealed a high correlation with $R = -0.99$.

As the pK shift of Asp170 may affect the electrostatic potential around the residue and change the pK of other residues, which is considered as a secondary effect of the mutation, the secondary or higher effect may be necessary to estimate the pI shift precisely. The precise evaluation of pI shift, however, is a complicated task and out of range of this paper. We did not evaluate the secondary effect quantitatively in this work and do not discuss about it in detail.

Fig. 4 shows the correlation plot of the activity vs. pI for the mutants and wild-type thermolysin. A clear negative correlation ($R = -0.99$) can be seen in these parameters. It may not seem to be easy to understand that the overall electrostatic property such as pI relates to the enzymatic activity directly, and it may suggest that there is a hidden mechanism that relates both the pI and the activity.

As pI shift is caused by the pK shifts of the ionizable residues, the negative correlation may suggest that the pK shift of some residues affects the activity. One of the candidates whose pK are affected by the mutation at the 213th site and whose pK shift affect the enzymatic activity strongly may be Asp170 whose side chain makes a hydrogen bond with that of

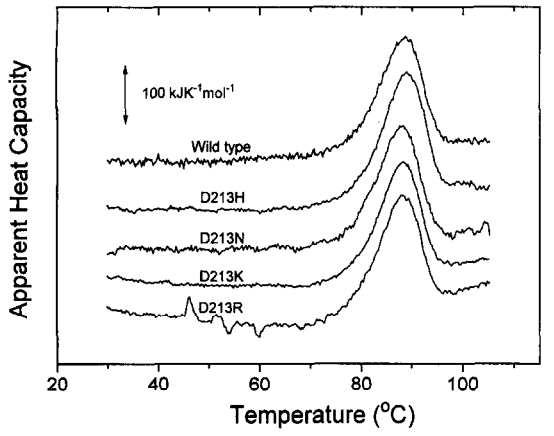

Fig. 5. Comparison of the thermal stability. The thermal stability of the mutants and wild-type thermolysin is measured with the differential scanning calorimetry device, MCS (MicroCal). Each chart is a single trace from 10°C to 105°C at the rate of 1 K/min. The sample buffer used is 50 mM HEPES (pH 8.28) containing 10 mM $CaCl_2$ and 0.1 μM $ZnSO_4$.

His142 that coordinates to the zinc ion at the active site.

3.5. Thermal stability of the mutants

In the previous paper we reported that another series of thermolysin mutants lost their thermal stability upon the single substitution at the 119th site [29], and concluded that the stability is largely influenced by a hydrogen bond broken by the mutation. On the other hand, the electrostatic contribution to the stability of the previous study was not obvious.

We have found that the series of D213-replaced thermolysins has almost the same thermal stability with wild-type enzyme (Fig. 5). Even the drastic amino acid replacement from acidic to basic amino acids has little influence on the thermal stability of thermolysin. It indicates that these replacements do not perturb its unfolding process.

Acknowledgements

We thank Dr. Haruki Nakamura for his kind permission to use his program. Fruitful discussions with Dr. Takuya Takahashi is gratefully acknowledged. This research was supported in part by the Special Coordination Funds of the Science and Technology Agency of Japanese Government and grants from the Ministry of Education, Science and Culture in Japan.

References

[1] S. Endo, J. Ferment. Technol., 40 (1962) 346.
[2] H. Matsubara, Methods Enzymol., 47 (1977) 642.
[3] K. Titani, M.A. Hermodson, L.H. Ericsson, K.A. Walsh and H. Neurath, Biochemistry, 11 (1972) 2427.
[4] K. Titani, M.A. Hermodson, L.H. Ericsson, K.A. Walsh and H. Neurath, Nat. New Biol., 238 (1972) 35.
[5] M.A. Holmes and B.W. Matthews, J. Mol. Biol., 160 (1982) 623.
[6] F.W. Dahlquist, J.W. Long and W.L. Bigbee, Biochemistry, 15 (1976) 1103.
[7] W.R. Kester and B.W. Matthews, Biochemistry, 16 (1977) 2506.
[8] W.R. Kester and B.W. Matthews, J. Biol. Chem., 252 (1977) 7704.
[9] M.A. Holmes and B.W. Matthews, Biochemistry, 20 (1981) 6912.
[10] D.G. Hangauer, B.W. Monzingo and B.W. Matthews, Biochemistry, 23 (1984) 5730.
[11] H.M. Holden, D.E. Tronrud, A.F. Monzingo, L.H. Weaver and B.W. Matthews, Biochemistry, 26 (1987) 8542.
[12] M. Takagi, T. Imanaka and S. Aiba, J. Bacteriol., 163 (1985) 824.
[13] M. Kubo and T. Imanaka, J. Gen. Microbiol., 134 (1988) 1883.
[14] N. Vasantha, L.D. Thompson, C. Rhodes, C. Banner, J. Nagle and D. Filpula, J. Bacteriol., 159 (1984) 811.
[15] L.F. Wang and R.J. Devenish, J. Gen. Microbiol., 139 (1993) 343.
[16] M.Y. Yang, E. Ferrari and D.J. Henner, J. Bacteriol., 160 (1984) 15.
[17] S. Toma, S. Campagnoli, E. De Gregoriis, R. Gianna, I. Margarit, M. Zamai and G. Grandi, Protein Eng., 2 (1989) 359.
[18] V.G.H. Eijsink, G. Vriend, B.V.D. Burg, J.R.V.D. Zee, O.R. Veltman, B.K. Stulp and G. Venema, Protein Eng., 5 (1992) 157.
[19] V.G.H. Eijsink, G. Vriend, B.V.D. Burg, J.R.V.D. Zee and G. Venema, Protein Eng., 5 (1992) 165.
[20] M. Kubo, Y. Mitsuda, M. Takagi and T. Imanaka, Appl. Environ. Microbiol., 48 (1992) 3779.
[21] I. Margarit, S. Campagnoli, F. Frigerio, G. Grandi, V.D. Filippis and A. Fontana, Protein Eng., 5 (1992) 543.
[22] F. Hardy, G. Vriend, O.R. Veltman, B.V.D. Vinne, G. Venema and V.G.H. Eijsink, FEBS Lett., 317 (1993) 89.
[23] R. Marquardt, R. Hilgenfeld and R. Keller, Eur. Pat. Appl. EP0418625A1 (1989).

[24] M.J. O'Donohue, B.P. Roques and A. Beaumont, Biochem. J., 300 (1994) 599.
[25] Y. Miki, J. Ferm. Bioeng., 77 (1994) 457.
[26] A.J. Russell, P.G. Thomas and A.R. Fersht, J. Mol. Biol., 193 (1987) 803.
[27] M.K. Gilson and B.H. Honig, Nature, 330 (1987) 84.
[28] M.J.E. Sternberg, F.R.F. Hayes, A.J. Russell, P.G. Thomas and A.R. Fersht, Nature, 330 (1987) 86.
[29] S. Kidokoro, Y. Miki, K. Endo, A. Wada, H. Nagao, T. Miyake, A. Aoyama, T. Yoneya, K. Kai and S. Ooe, FEBS Lett., 367 (1995) 73.
[30] S. Kidokoro, Y. Miki, K. Endo and A. Wada, in A. Pullman et al. (Eds.), Modelling of Biomolecular Structures and Mechanisms, Kluwer, Dordrecht, 1995, p. 399.
[31] M.A. Vandeyar, M.P. Weiner, C.J. Hutton and C.A. Batt, Gene, 65 (1988) 129.
[32] M. Kubo and T. Imanaka, J. Bacteriol., 171 (1989) 4080.
[33] Y. Ohta, Y. Ogura and A. Wada, J. Biol. Chem., 241 (1966) 5919.
[34] J. Feder, Biochem. Biophys. Res. Commun., 32 (1968) 326.
[35] H. Nakamura and S. Nishida, J. Phys. Soc. Jpn., 56 (1987) 1609.
[36] T. Takahashi, H. Nakamura and A. Wada, Biopolymers, 32 (1992) 897.
[37] C. Tanford and R. Roxby, Biochemistry, 11 (1972) 2192.
[38] P.M. Colman, J.N. Jansonius and B.W. Matthews, J. Mol. Biol., 70 (1972) 701.